# Surface Instability of Sheared Soft Tissues

M. Destrade, M.D. Gilchrist,
D.A. Prikazchikov, G. Saccomandi

2008

**Abstract**

When a block made of an elastomer is subjected to large shear, its surface remains flat. When a block of biological soft tissue is subjected to large shear, it is likely that its surface in the plane of shear will buckle (apparition of wrinkles). One factor that distinguishes soft tissues from rubber-like solids is the presence – sometimes visible to the naked eye – of oriented collagen fibre bundles, which are stiffer than the elastin matrix into which they are embedded but are nonetheless flexible and extensible. Here we show that the simplest model of isotropic nonlinear elasticity, namely the incompressible neo-Hookean model, suffers surface instability in shear only at tremendous amounts of shear, i.e., above 3.09, which corresponds to a 72° angle of shear. Next we incorporate a family of parallel fibres in the model and show that the resulting solid can be either reinforced or strongly weakened with respect to surface instability, depending on the angle between the fibres and the direction of shear, and depending on the ratio $E/\mu$ between the stiffness of the fibres and that of the matrix. For this ratio we use values compatible with experimental data on soft tissues. Broadly speaking, we find that the surface becomes rapidly unstable when the shear takes place "against" the fibres, and that as $E/\mu$ increases, so does the sector of angles where early instability is expected to occur.

**Keywords:** soft tissues, large shear, extensible fibres, mechanical instability.

## 1 Introduction

Rubber-like solids and biological soft tissues can both be efficiently modelled within the framework of finite elasticity, which can account for large

deformations, physical nonlinearities, incompressibility, residual stresses, viscoelasticity, etc. One of the most salient differences between the two types of solids is that at rest, elastomers are essentially isotropic whilst soft tissues are essentially anisotropic, because of the presence of collagen fibre bundles. In that respect, it is worthwhile to consider the effect of incorporating families of parallel fibres into an isotropic matrix, and see if it can model some striking differences between the mechanical behaviour of elastomers and of soft tissues. Consider for instance the large shear of a solid block. When the block is made of an elastomer such as silicone, its surface remains stable; when it is made of a biological soft tissue such as skeletal muscle, its surface wrinkles for certain ranges of orientation between the direction of shear and the (presumed) direction of fibres, see Fig. 1. Here we show that one of the simplest models of anisotropic nonlinear elasticity, which requires only knowledge of the fibre/matrix stiffness ratio, is sufficient to successfully predict these behaviours.

To model the isotropic elastomer (Section 2), we take the incompressible neo-Hookean solid, and find that it does not suffer surface instability unless it is subjected to a substantial amount of shear (critical amount of shear: 3.09, critical angle of shear: 72°). In that case the wrinkles are aligned with the direction of greatest stretch. (The wrinkling analysis relies on the incremental theory of nonlinear elasticity, see for instance Biot [1] or Ogden [2]). Next, we introduce one family of parallel fibres into the model (Section 3). To model biological soft tissues with one preferred direction (Section 4), we take the incompressible neo-Hookean strain energy density, augmented by the so-called 'standard reinforcing model': this model has only two parameters, namely the shear modulus $\mu$ of the soft (neo-Hookean) matrix and the fibre stiffness $E$.

With respect to surface instability, only the ratio $E/\mu$ of these two quantities plays a role. We take it to be equal in turn to 40.0, 20.0, and 10.0, in agreement with the range of experimental measures found in the literature. We then find that when the angle between the direction of shear and the direction of the fibres is small, the solid is much more stable than the isotropic solid obtained in the absence of fibres; when the angle increases but is less than 99.0° (for $E/\mu = 40.0$), 102.8° (for $E/\mu = 20.0$), 108.1° (for $E/\mu = 10.0$), the solid remains more stable than the isotropic solid; however, when the angle exceeds those values, the critical amount of shear for surface instability drops to extremely low levels, indicating the appearance of wrinkles as soon as shearing occurs. In that case, the wrinkles are found to be almost orthogonal to the fibres, in accordance with visual observations.

It is hoped that the paper provides a greater understanding of the causes of certain instabilities in soft tissues and a quantitative tool to measure what

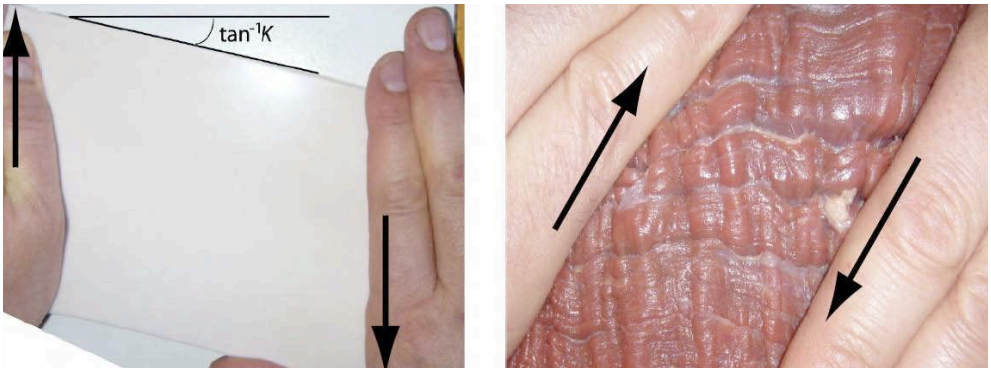


Figure 1: Shearing (along the arrows) a block of silicone of approximate size 15cm × 10cm × 1.5cm and a block of mammalian skeletal muscle (beef) of approximate size 15cm × 10cm × 3cm; one does not exhibit surface instability, the other does.

deformations (critical amounts of shear) are permissible and in which directions. Surface instability has a direct connection to slab and tube buckling, which in biomechanics may potentially translate into aneurysms formation, arterial kinking and tortuosity, brain trauma, and many other, still not well understood, pathologies.

## 2 Surface instability of a sheared isotropic solid

First, we recall known results in the theory of surface wrinkling valid for *isotropic* solids.

Consider a semi-infinite body made of an incompressible isotropic neo-Hookean solid, for which the strain energy function $W$, written as a function of the principal stretch ratios $\lambda_1$, $\lambda_2$, $\lambda_3$, is given by

$$W = \mu(\lambda_1^2 + \lambda_2^2 + \lambda_3^2 - 3)/2. \tag{1}$$

Here $\mu$ is the shear modulus, and $\lambda_1\lambda_2\lambda_3 = 1$ by the incompressibility constraint. Then subject the solid to a large homogeneous static deformation, such that $\lambda_2$ is the stretch ratio along the normal to the free surface. It has long been known that the surface becomes unstable when the following *wrinkling condition* is met,

$$\lambda_1^2\lambda_3 = \sigma_0, \tag{2}$$

where $\sigma_0 \simeq 0.296$ is the real root of $\sigma^3+\sigma^2+3\sigma-1 = 0$ (Green and Zerna [3], Biot [1]).

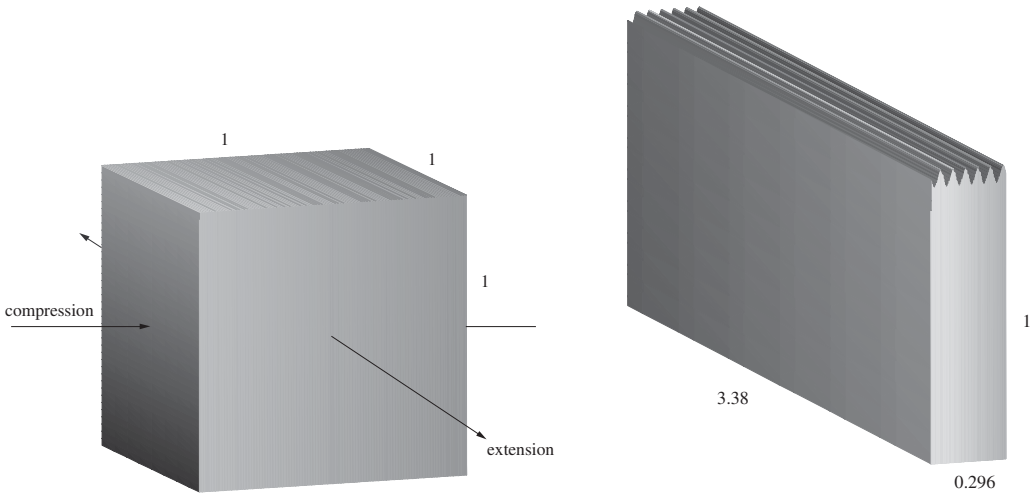


Figure 2: Large plane strain deformation of a unit cube near the surface of a semi-infinite incompressible neo-Hookean solid. When the solid is compressed by 71% (or equivalently, stretched by 238%), its surface wrinkles. Note that the analysis quantifies neither the amplitude nor wavelength of the wrinkles.

In the following *plane strain* situation,

$$\lambda_1 = \lambda, \qquad \lambda_2 = 1, \qquad \lambda_3 = \lambda^{-1}, \tag{3}$$

the critical stretch of compression found from Eq. (2) is clearly $\lambda_1 = \sigma_0 \simeq 0.296$ (and then $\lambda_3 = \sigma_0^{-1} \simeq 3.38$). The conclusion is that when a semi-infinite neo-Hookean solid, which is neither allowed to expand nor contract along the normal to its boundary, is *compressed* by 71% in a given direction (lying in the boundary), it buckles with wrinkles developing along the direction *orthogonal* to the direction of compression. Equivalently, when it is *stretched* by 238%, it buckles with wrinkles *parallel* to the direction of tension. Figure 2 summarizes these results.

It is natural to wonder whether the surface might have become unstable in other directions earlier, that is at compressive ($\leqslant 1$) ratios larger than 0.296, or at tensile ($\geqslant 1$) ratios smaller than 3.38. Flavin [4] shows that wrinkles develop parallel to the direction making an angle $\theta$ with the principal direction of strain associated with the stretch ratio $\lambda_3$ when the following wrinkling condition is met

$$\lambda_1^2\lambda_3^2(\lambda_1^2\cos^2\theta + \lambda_3^2\sin^2\theta) = \sigma_0^2. \tag{4}$$

In the plane strain situation Eq. (3), this condition is quadratic in $\lambda^2$,

$$\lambda^4\cos^2\theta - \lambda^2\sigma_0^2 + \sin^2\theta = 0. \tag{5}$$

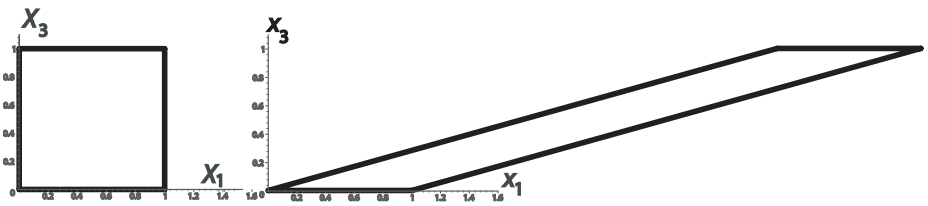


Figure 3: Large simple shear of a unit square in the surface of a semi-infinite incompressible neo-Hookean solid. When the solid is sheared by an amount $K_0 \simeq 3.09$ (Figure on the right), its surface wrinkles. The corresponding angle of shear is $\tan^{-1} K_0 \simeq 72.0°$, which physically, is abnormaly large. Then the wrinkles are parallel to the direction of greatest tension, which makes an angle $\varphi_0 \simeq 16.5°$ with the direction of shear (and so, the wrinkles are almost aligned with the sheared faces.)

It has real roots provided $\theta$ is in the ranges $-\theta_0 \leqslant \theta \leqslant \theta_0$ or $\pi/2 - \theta_0 \leqslant \theta \leqslant \pi/2 + \theta_0$, where $\theta_0 = (1/2)\sin^{-1}\sigma_0^2 \simeq 2.51°$. In the former range, the compressive critical stretch found from the biquadratic Eq. (5) turns out to be smaller than 0.296 and in the latter range, to be larger than 3.38. Thus surface instability for plane strain Eq. (3) occurs when the isotropic neo-Hookean half-space is in compression at a ratio $\sigma_0$ or equivalently, in tension at a ratio $\sigma_0^{-1}$. The *wrinkles are parallel to the direction of greatest stretch* and orthogonal to the direction of greatest compression.

Now *simple shear* belongs to the family of plane strains Eq. (3), with the following connection between the principal stretches and the amount of shear $K$ (see Ogden [2]) for instance),

$$K = \lambda - \lambda^{-1}, \qquad \lambda = K/2 + \sqrt{1 + K^2/4}. \tag{6}$$

Also, the *direction of greatest stretch* is at an angle $\psi$ with the direction of shear, where $\psi \in ]0, \pi/4]$ is given by

$$\tan 2\psi = 2/K. \tag{7}$$

Clearly $\lambda > 1$ here, and so surface shear instability occurs in tension, when the amount of shear is equal to $K_0 = \sigma_0^{-1} - \sigma_0 \simeq 3.09$. The corresponding critical angle of shear is then $\tan^{-1} K_0 \simeq 72.0°$, see Fig. 3. This is quite large shear.

# 3 Sheared fibre-reinforced solids

## 3.1 Finite simple shear

Now we consider a semi-infinite composite incompressible solid, made of an isotropic matrix reinforced with one family of parallel extensible fibres, themselves parallel to the boundary of the solid. In the undeformed configuration, we call $(X_1, X_2, X_3)$ the set of Cartesian coordinates such that the solid is located in the $X_2 \geqslant 0$ region. We denote by $\boldsymbol{E}_1$, $\boldsymbol{E}_2$, $\boldsymbol{E}_3$ the orthogonal unit vectors defining the Lagrangian (reference) axes, aligned with the $X_1$, $X_2$, $X_3$ directions, respectively.

When the solid is sheared in the direction of $\boldsymbol{E}_1$, the particle at $\boldsymbol{X}$ moves to its current position $\boldsymbol{x}$. We call $\boldsymbol{F} = \partial \boldsymbol{x}/\partial \boldsymbol{X}$ the associated deformation gradient tensor, and $\boldsymbol{B} = \boldsymbol{F}\boldsymbol{F}^T$ the left Cauchy-Green strain tensor. We then call $(x_1, x_2, x_3)$ the Cartesian coordinates, aligned with $(X_1, X_2, X_3)$, corresponding to the current position $\boldsymbol{x}$. In the current configuration, the basis vectors are $\boldsymbol{e}_1$, $\boldsymbol{e}_2$, $\boldsymbol{e}_3$, and here they are such that $\boldsymbol{e}_i \equiv \boldsymbol{E}_i$ $(i = 1, 2, 3)$. The *simple shear* of amount $K$ is described by

$$x_1 = X_1 + KX_3, \qquad x_2 = X_2, \qquad x_3 = X_3. \tag{8}$$

We thus find in turn that

$$\boldsymbol{F} = \boldsymbol{I} + K\boldsymbol{e}_1 \otimes \boldsymbol{E}_3, \qquad \boldsymbol{B} = \boldsymbol{I} + K(\boldsymbol{e}_1 \otimes \boldsymbol{e}_3 + \boldsymbol{e}_1 \otimes \boldsymbol{e}_3) + K^2 \boldsymbol{e}_1 \otimes \boldsymbol{e}_1. \tag{9}$$

The principal stretches are given by Eq. (3) and Eq. (6), and the first principal isotropic invariant $I_1 = \text{tr } \boldsymbol{B}$ is given here by

$$I_1 = 3 + K^2. \tag{10}$$

Note that for shear, the second principal isotropic invariant, $I_2 = [I_1^2 - \text{tr } (\boldsymbol{B}^2)]/2$ is also equal to $3 + K^2$.

## 3.2 One family of fibres

For solids reinforced with one family of parallel fibres lying in the plane of shear, we work in all generality and consider that the angle $\Phi$ (say) between the fibres and the $X_1$ direction can take any value. In other words, the unit vector $\boldsymbol{M}$ (say) in the preferred fibre direction has components

$$\boldsymbol{M} = \cos\Phi \boldsymbol{E}_1 + \sin\Phi \boldsymbol{E}_3, \tag{11}$$

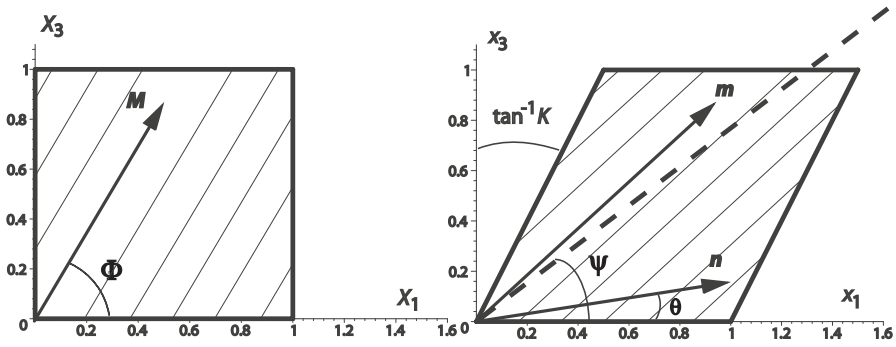


Figure 4: A unit square lying on the surface of a semi-infinite solid reinforced with one family of fibres (thin lines) and subject to a simple shear of amount $K = 0.5$ (angle of shear is $\tan^{-1} K \simeq 26.6°$) in the $X_1$ direction. In the reference configuration, the fibres are along the unit vector $\boldsymbol{M}$, at the angle $\Phi = 60°$ with the $X_1$-axis. In the current configuration, they are along $\boldsymbol{m}$. The unit vector $\boldsymbol{n}$ is orthogonal to the wrinkles' front (when they exist). Finally, the dashed line is aligned with the direction of greatest stretch; it is at an angle $\psi \simeq 38°$ to the direction of shear.

in the reference configuration. Simple shear is a homogeneous deformation, and so $\boldsymbol{M}$ is transformed into $\boldsymbol{m} = \boldsymbol{F}\boldsymbol{M}$ in the current configuration, that is

$$\boldsymbol{m} = (\cos\Phi + K\sin\Phi)\boldsymbol{e}_1 + \sin\Phi\boldsymbol{e}_3. \tag{12}$$

Without loss of generality, we take the ranges $K \geqslant 0$, $0 \leqslant \Phi \leqslant \pi$, which cover all possible orientations of the fibres with respect to the direction of shear.

To fix the ideas, consider Fig. 4. There we shear the half-space by a finite amount $K = 0.5$, in the direction making an angle $\Phi = 60°$ with the fibres. Notice that a unit vector $\boldsymbol{n}$ making an angle $\theta$ with the direction of shear is also represented in the current configuration. This is the normal to the wrinkles' front; in the next section we look for surface wrinkles in all directions (the angle $\theta$ spans the interval $[0°, 180°]$) and we determine which is the smallest corresponding critical amount of shear.

Finally we introduce the anisotropic invariants $I_4 \equiv \boldsymbol{m}\cdot\boldsymbol{m}$ and $I_5 \equiv \boldsymbol{F}\boldsymbol{m}\cdot\boldsymbol{F}\boldsymbol{m}$; in particular we find

$$I_4 = 1 + K\sin 2\Phi + K^2\sin^2\Phi. \tag{13}$$

Recall that $I_4$ is the squared stretch in the fibre direction [5]. In particular, if $I_4 \geqslant 1$ then the fibres are in extension, and if $I_4 \leqslant 1$ then they are in compression. Clearly here, when $0 \leqslant \Phi \leqslant \pi/2$, the fibres are always in

extension but when $\pi/2 < \Phi < \pi$, there exist a certain amount of shear (explicitly, $-2/\tan\Phi$) below which the fibres are in compression.

### 3.3 Constitutive assumptions

In general, the strain-energy density $W$ of a hyperelastic incompressible solid reinforced with one family of parallel extensible fibres depends on the isotropic invariants $I_1$ and $I_2$, and on the anisotropic invariants (Spencer [5]) $I_4$ and $I_5$. We assume that $W$ is the sum of an isotropic part and an anisotropic part. For the isotropic part, modelling the properties of the 'soft' matrix, we take the neo-Hookean strain-energy density in order to make a connection with the results of Section 2. For the anisotropic part, modelling the properties of the extensible 'stiff' fibres, we take a function of $I_4$ only, say $F(I_4)$. Hence, we restrict our attention to those solids with strain energy density

$$W = \mu(I_1 - 3)/2 + F(I_4). \tag{14}$$

This assumption is quite common in the biomechanics literature. Although it does not prove crucial to the analysis, it leads to compact and revealing expressions (Note that the consideration of a more general $W$ poses no major extra difficulty, but results in much longer expressions.).

The corresponding Cauchy stress tensor $\boldsymbol{\sigma}$ is (see e.g. [6]): $\boldsymbol{\sigma} = -p\boldsymbol{I} + \mu\boldsymbol{B} + 2F'(I_4)\boldsymbol{m}\otimes\boldsymbol{m}$, where $p$ is a Lagrange multiplier introduced by the constraint of incompressibility. The surface $x_2 = 0$ is free of tractions: here $\sigma_{12} = \sigma_{23} = 0$ follows from $B_{12} = B_{23} = 0$ and $\boldsymbol{m}\cdot\boldsymbol{e}_2 = 0$ (see Eq. (9) and Eq. (12)), whilst $\sigma_{22} = 0$ gives $p = \mu$. Thus, the pre-stress necessary to maintain the shear Eq. (8) is

$$\boldsymbol{\sigma} = \mu(\boldsymbol{B} - \boldsymbol{I}) + 2F'(I_4)\boldsymbol{m}\otimes\boldsymbol{m}, \tag{15}$$

showing that the directions of principal stress and strain do not coincide in general (except when the preferred direction is aligned with principal directions of strain).

## 4 Surface instability

### 4.1 Incremental deformations

We seek solutions to the incremental equations of equilibrium and incremental boundary conditions in the form of a sinusoidal perturbations whose amplitude decays rapidly with depth. In contrast to the isotropic case of

Section 2, we do not know a priori in which direction the wrinkles should be aligned, and we take the normal to the wrinkles' front $\boldsymbol{n}$ (say) to lie in the $(x_1x_3)$ plane at an arbitrary angle $\theta$ with $x_1$, see Fig. 4. Hence, we seek a perturbation solution $\boldsymbol{u}$ (mechanical displacement) and $\dot{p}$ (increment of the Lagrange multiplier associated with incompressibility) in the form,

$$\{\boldsymbol{u}, \dot{p}\} = \{\boldsymbol{U}(kx_2), \mathrm{i}kP(kx_2)\}\mathrm{e}^{\mathrm{i}k(\cos\theta x_1 + \sin\theta x_3)}, \tag{16}$$

where $k$ is the "wave"-number and $\boldsymbol{U}$, $P$ are functions of $kx_2$ alone.

The incremental equations read

$$s_{ji,j} = 0, \qquad u_{j,j} = 0, \tag{17}$$

where the comma denotes partial differentiation with respect to $x_j$, and $\boldsymbol{s}$ is the incremental nominal stress tensor. Its components are [2],

$$s_{ji} = \mathcal{A}_{0jilk}u_{k,l} + pu_{j,i} - \dot{p}\delta_{ij}, \tag{18}$$

where $\boldsymbol{\mathcal{A}_0}$ is the fourth-order tensor of instantaneous elastic moduli. In general it has a long expression for fibre-reinforced solids, with possibly 45 non-zero components, see for example [7, 8]. For $W$ in the form Eq. (14), $\boldsymbol{B}$ by Eq. (9), and $\boldsymbol{M}$ by Eq. (11), we find the following components

$$\mathcal{A}_{0jilk} = \mu\delta_{ik}B_{jl} + 2F'(I_4)\delta_{ik}m_jm_l + 4F''(I_4)m_im_jm_km_l \tag{19}$$

see Merodio and Ogden [9]. Clearly, these components have the symmetries $\mathcal{A}_{0jilk} = \mathcal{A}_{0lkji}$ and $\mathcal{A}_{0jilk} = \mathcal{A}_{0jkli}$. We end up with 23 non-zero components, several of which are equal to one another (*in toto* there are 13 different components).

Clearly, if $\boldsymbol{u}$ and $\dot{p}$ are of the form Eq. (16), then by Eq. (18) the $s_{ji}$ are of a similar form, say

$$s_{ji} = \mathrm{i}kS_{ji}(kx_2)\mathrm{e}^{\mathrm{i}k(\cos\theta x_1 + \sin\theta x_3)}, \tag{20}$$

where the $S_{ji}$ are functions of the variable $kx_2$ only. By a systematic procedure, first laid down by Chadwick [10] (see also [11–14]), we can eliminate $P$ and write the incremental equations of equilibrium as a first-order differential system. This is known as the *Stroh formulation* of the problem,

$$\begin{bmatrix}\boldsymbol{U}' \\ \boldsymbol{S}'\end{bmatrix} = \mathrm{i}\boldsymbol{N}\begin{bmatrix}\boldsymbol{U} \\ \boldsymbol{S}\end{bmatrix}, \quad \text{where} \quad \boldsymbol{U} = \begin{bmatrix}U_1 \\ U_2 \\ U_3\end{bmatrix}, \quad \boldsymbol{S} = \begin{bmatrix}S_{21} \\ S_{22} \\ S_{23}\end{bmatrix}, \quad \boldsymbol{N} = \begin{bmatrix}\boldsymbol{N}_1 & \boldsymbol{N}_2 \\ \boldsymbol{N}_3 & \boldsymbol{N}_1\end{bmatrix}, \tag{21}$$

and the symmetric $3 \times 3$ matrices $\boldsymbol{N}_1$, $\boldsymbol{N}_2$, $\boldsymbol{N}_3$ are given by

$$-\boldsymbol{N}_1 = \begin{bmatrix} 0 & \cos\theta & 0 \\ \cos\theta & 0 & \sin\theta \\ 0 & \sin\theta & 0 \end{bmatrix}, \quad \boldsymbol{N}_2 = \begin{bmatrix} 1/\mu & 0 & 0 \\ 0 & 0 & 0 \\ 0 & 0 & 1/\mu \end{bmatrix}, \quad -\boldsymbol{N}_3 = \begin{bmatrix} \eta & 0 & \kappa \\ 0 & \nu & 0 \\ \kappa & 0 & \chi \end{bmatrix}, \tag{22}$$

with

$$\begin{aligned} \eta &= (\mathcal{A}_{01111} + 3\mu)\cos^2\theta + 2\mathcal{A}_{01131}\cos\theta\sin\theta + \mathcal{A}_{03131}\sin^2\theta, \\ \nu &= \mathcal{A}_{01212}\cos^2\theta + 2\mathcal{A}_{01232}\cos\theta\sin\theta + \mathcal{A}_{03232}\sin^2\theta - \mu, \\ \chi &= \mathcal{A}_{01313}\cos^2\theta + 2\mathcal{A}_{01333}\cos\theta\sin\theta + (\mathcal{A}_{03333} + 3\mu)\sin^2\theta, \\ \kappa &= \mathcal{A}_{01113}\cos^2\theta + (2\mathcal{A}_{01133} + 3\mu)\cos\theta\sin\theta + \mathcal{A}_{03133}\sin^2\theta. \end{aligned} \tag{23}$$

Notice how all the information relative to anisotropy is located in the $\boldsymbol{N}_3$ matrix.

The solution to the system Eq. (21) is clearly an exponential

$$\{\boldsymbol{U}, \boldsymbol{S}\} = \{\boldsymbol{U}^0, \boldsymbol{S}^0\}\mathrm{e}^{\mathrm{i}kqx_2}, \tag{24}$$

where $\boldsymbol{U}^0, \boldsymbol{S}^0$ are constant vectors and $q$ is an eigenvalue of $\boldsymbol{N}$. The characteristic equation associated with $\boldsymbol{N}$ is a *bicubic* [8],

$$q^6 - \left(2 - \frac{\chi + \eta}{\mu}\right) q^4 + \left(1 + \frac{\nu - 2\epsilon}{\mu} + \frac{\chi\eta - \kappa^2}{\mu^2}\right) q^2 + \frac{\epsilon(\mu + \nu)}{\mu^2} = 0, \tag{25}$$

where the quantity $\epsilon$ is defined by

$$\epsilon = \chi\cos^2\theta - 2\kappa\cos\theta\sin\theta + \eta\sin^2\theta. \tag{26}$$

The existence of real roots to this equation corresponds to the loss of ellipticity of the governing equations (*material* instabilities). This possibility has been thoroughly investigated before, see [9,15,16]. Here we focus on complex roots and keep those satisfying $\mathrm{Im}q > 0$ , for a surface-type bifurcation which decays with depth (*geometric* instability).

## 4.2 Wrinkling condition and resolution scheme

Over the years, many schemes have been developed to solve surface boundary problems using the Stroh formulation; we used in turn the determinantal method [17], the Riccati matrix equation of surface impedance [13, 14], and explicit polynomial equations [18], in order to double-check our numerical computations.

The crucial boundary condition is to find the amount of shear at which the surface of the sheared solid is free of tractions. The safest way to express this is

$$\det \boldsymbol{Z} = 0, \tag{27}$$

where $\boldsymbol{Z}$ is the (Hermitian) *surface impedance matrix*, which relates tractions to displacements through $\boldsymbol{S} = \mathrm{i}\boldsymbol{Z}\boldsymbol{U}$. We remark that the schemes are not as safe in surface stability problems as they are in surface wave theory because of incompressibility [13, 14] and non-monotonicity of $\det \boldsymbol{Z}$ with $K$.

Once Eq. (27) is reached, we can construct an incremental solution to the equations of equilibrium which is adjacent to the large shear equilibrium, and signals the onset of surface instability. We adopted the following strategy:

*(i)* Fix $\Phi$, the angle between the direction of shear and the preferred direction;

*(ii)* Fix $\theta$, the angle between the direction of shear and the normal to the wrinkles' front;

*(iii)* Find (if it exists) the corresponding critical amount of shear such that Eq. (27) is satisfied.

Then repeat Steps *(ii)* and *(iii)* for other angles $\theta$ until the entire surface is spanned, and keep the smallest critical amount of shear $K_{\mathrm{cr}}$ (say) for the angle $\Phi$ chosen in Step *(i)*. Then take a different value of $\Phi$, until all possible fibre orientations are covered. *In fine* a graph of $K_{\mathrm{cr}}$ as a function of $\Phi$ is generated.

# 5 Numerical results for biological soft tissues

We take the *standard reinforcing model*,

$$W = \mu(I_1 - 3)/2 + E(I_4 - 1)^2/4, \tag{28}$$

where $E$ is an extensional modulus in the fibre direction. This model has been used for several soft tissues, such as papillary muscle [19], myocardium [19], skeletal muscles [20], or brainstem [21].

That latter reference examines the ability of the constitutive model Eq. (28) to describe the mechanical response of porcine brainstem specimens. Recall that large deformations, in particular large shears, of brain tissue are often associated with traumatic brain injuries (Doorly and Gilchrist, 2006). Ning et al. [21] find that the model provides good agreement with experimental data; they estimate that for 4 week old pigs, $E$ is about 20 times larger than

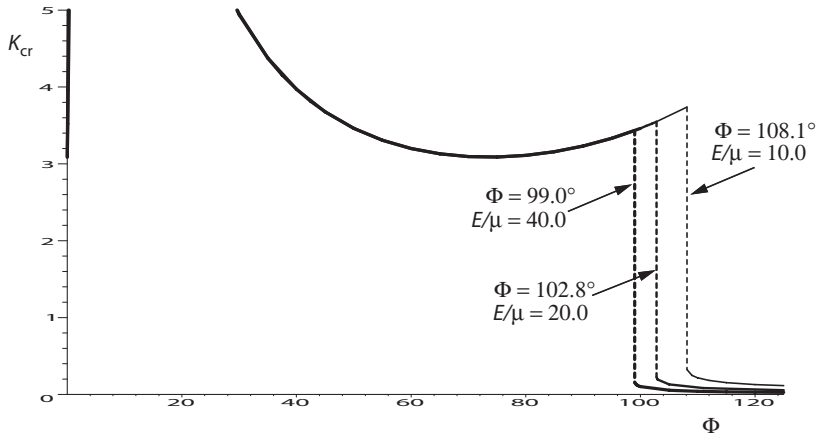


Figure 5: Variations of the critical amount of shear for surface instability with the angle between the directions of shear and the fibres. The solid is modelled as a neo-Hookean matrix reinforced with one family of fibres (standard reinforcing model); the ratio of the matrix shear modulus to the fibre stiffness is taken in turn as 40.0, 20.0, and 10.0. The 3 graphs coincide as long as $0 < \Phi < \Phi_0$, where $\Phi_0 = 99.0°$, $102.8°$, $108.1°$, respectively. At $\Phi \simeq \Phi_0$, the half-space switches from being very stable ($K_{\rm cr} > 3.09$) to being easily unstable ($K_{\rm cr} < 0.3$). The part of the plot corresponding to $K_{\rm cr} > 5$ is not shown for physical and visual reasons.

$\mu$. In a recent review on physical properties of tissues for arterial ultrasound, Hoskins [23] emphasizes the need for constitutive models of nonlinear elastic behavior. He also collects available data for arterial walls: in particular for abdominal aortic aneurysms, ex vivo measurements indicate that $E$ is about 10 times larger than $\mu$ whilst for human atherosclerotic plaque, $E$ seems to be more than 40 times $\mu$. For our numerical computations we take in turn the values $E/\mu = 40.0$, 20.0, 10.0, and collect the corresponding results on Fig. 5.

Broadly speaking, we find a region where the solid is strongly reinforced by the family of fibres, followed by an abrupt drop in the value of the critical amount of shear for surface instability, which occurs earlier as $E/\mu$ increases.

When the fibres are aligned with the direction of shear, they are not stretched and they play no role; thus it is appropriate that at $\Phi = 0.0°$, we find $K_{\rm cr} = 3.09$, the critical amount of shear for an isotropic neo-Hookean half-space, see Section 2.

Next we find that $K_{\rm cr}$ shoots up to unrealistic values when $\Phi \gtrsim 0.0°$: for instance $K_{\rm cr} = 32.48$ when $\Phi = 3.0°$ (not represented for visual convenience). Hence, the solid is strongly reinforced with respect to surface stability when

the shear takes place more or less along the fibres: wrinkling is prevented.

As the angle $\Phi$ between the shear and the fibres increases, the critical amount of shear goes through a maximum, then a minimum, always remaining above 3.09, the value for an isotropic neo-Hookean half-space, as long as $\Phi \leqslant \Phi_0$, where $\Phi_0 = 99.0°$, $102.8°$, $108.1°$, approximatively, for $E/\mu = 40.0, 20.0, 10.0$, respectively. It is worth noting that in the range $90.0° < \Phi < \Phi_0$, the fibres undergo a slight compression at low shear levels, and then are in extension until the critical amount of shear is reached; even when the fibres are compressed, the half-space remains stable.

When the angle $\Phi$ is large, $\Phi_0 < \Phi < 180.0°$, the half-space becomes unstable at low amounts of shear. For instance at $\Phi = 99.07°$, we find that $K_{\rm cr} = 0.153$ when $E/\mu = 40.0$; note that in reaching that critical amount of shear, the fibres are compressed by less than 1.3%. The switch from high to low critical amounts of shear is abrupt, due to the non-monotonicity of $\det \boldsymbol{Z}$ with $K$: this quantity has a minimum in the high range ($K > 3.09$) which is always negative (indicating the existence of a root to Eq. (27)), but it can also have a minimum in the low range ($K < 0.3$). This minimum is positive when $\Phi < \Phi_0$ (no root to Eq. (27)) but negative when $\Phi > \Phi_0$, hence the jump in $K_{\rm cr}$.

Finally we note that in the range $\Phi_0 < \Phi < 180.0°$, the angle $\theta$ normal to the wrinkles' front is close to $\Phi$ (within 2°), indicating that the wrinkles are almost at right-angle with the fibres; these predictions are in accordance with the observation of Fig. 1.

# 6 Discussion

We developed a quantitative methodology to understand the formation of wrinkles in some biological soft tissues. The analysis allowed us to model some visual observations of a sheared elastomer versus a sheared piece of skeletal muscle, based on a simple nonlinear anisotropic constitutive law (requiring the knowledge of only one quantity, $E/\mu$).

Studying the geometry and mechanics of wrinkles is relevant to many biomechanical applications such as for instance the treatment of scars, and our results may provide some help in developing rational approaches to these problems. The next logical step is to apply and generalize this methodology to model the wrinkling of skin and other biological membranes. These may require more work than here, with the consideration of two families of parallel fibres (the collagen network), but the methodology remains essentially the same. It is also exact, versatile, and more convenient to apply than methods based on approximate theories (e.g. Föppl-von Kármán plate equations)

because it can accommodate easily anisotropy, nonlinear constitutive laws, finite thickness, and large homogeneous pre-deformation.

# References


[1] Biot, M. A., 1963, "Surface Instability of Rubber in Compression," Applied Science Research, A12, pp. 168–182.

[2] Ogden, R. W., 1984, Non-Linear Elastic Deformations. Ellis Horwood, Chichester.

[3] Green, A. E., and Zerna, W., 1954, Theoretical Elasticity, University Press, Oxford.

[4] Flavin, J. N., 1963, "Surface Waves in Pre-Stressed Mooney Material," Quarterly Journal of Mechanics and Applied Mathematics, 16, pp. 441–449.

[5] Spencer, A. J. M., 1984, Continuum Theory of the Mechanics of Fiber Reinforced Composites, CISM 282, Springer, New York.

[6] Ogden, R. W., 2003, Non-Linear Elasticity with Application to Material Modelling. Institute of Fundamental Technological Research, Warsaw.

[7] Chadwick, P., and Whitworth, A. M., 1986, "Exceptional Waves in a Constrained Elastic Body," Quarterly Journal of Mechanics and Applied Mathematics, 39, pp. 309–325.

[8] Prikazchikov, D. A., and Rogerson, G.A., 2004, "On Surface Wave Propagation in Incompressible, Transversely Isotropic, Pre-Stressed Elastic Half-Spaces," International Journal of Engineering Science, 42, pp. 967–986.

[9] Merodio, J., and Ogden, R. W., 2002, "Material Instabilities in Fiber-Reinforced Nonlinearly Elastic Solids Under Plane Deformation," Archives of Mechanics, 54, pp. 525–552.

[10] Chadwick, P., 1997. "The Application of the Stroh Formalism to Prestressed Elastic Media," Mathematics and Mechanics of Solids, 97, pp. 379–403.

[11] Destrade, M., and Ogden, R. W., 2005. "Surface Waves in a Stretched and Sheared Incompressible Elastic Material," International Journal of Non-Linear Mechanics, 40, pp. 241–253.

[12] Destrade, M., Otténio, M., Pichugin, A. V., and Rogerson, G.A., 2005, "Non-Principal Surface Waves in Deformed Incompressible Materials," International Journal of Engineering Science, 43, pp. 1092–1106.

[13] Fu, Y. B., 2005a, "An Explicit Expression for the Surface-Impedance Matrix of a Generally Anisotropic Incompressible Elastic Material in a State of Plane Strain," International Journal of Non-Linear Mechanics, 40, pp. 229–239.

[14] Fu, Y. B., 2005b, "An Integral Representation of the Surface-Impedance Tensor for Incompressible Elastic Materials," Journal of Elasticity, 81, pp. 75–90.

[15] Triantafyllidis, N., and Abeyaratne, R., 1983, "Instabilities of a Finitely Deformed Fiber-Reinforced Elastic Material," ASME Journal of Applied Mechanics, 50, pp. 149–156.

[16] Qiu, G. Y., and Pence, T. J., 1997, "Loss of Ellipticity in Plane Deformation of a Simple Directionally Reinforced Incompressible Nonlinearly Elastic Solid," Journal of Elasticity, 49, pp. 31–63.

[17] Farnell, G. W., 1970, "Properties of Elastic Surface Waves," In: Mason, W. P., Thurston, R. N. (Eds.), Physical Acoustics Volume 6. Academic Press, New York, pp. 109–166.

[18] Destrade, M., 2005, "On Interface Waves in Misoriented Pre-Stressed Incompressible Elastic Solids," IMA Journal of Applied Mathematics, 70, pp. 3–14.

[19] Taber, L. A., 2004, Nonlinear Theory of Elasticity. World Scientific, New Jersey.

[20] Röhrle, O., and Pullan, A. J., 2007, "Three-Dimensional Finite Element Modelling of Muscle Forces During Mastication," Journal of Biomechanics, 40, pp. 3363–3372.

[21] Ning, X., Zhu, Q., Lanir, Y., and Margulies, S. S., 2006, "A Transversely Isotropic Viscoelastic Constitutive Equation for Brainstem Undergoing Finite Deformation," ASME Journal of Biomechanical Engineering, 128, pp. 925–933.

[22] Doorly, M. C., and Gilchrist, M. D., 2006, "The Analysis of Traumatic Brain Injury Due to Head Impacts Arising from Falls Using Accident Reconstruction," Computer Methods in Biomechanics and Biomechanical Engineering, 9, pp. 371–377.

[23] Hoskins, P. R., 2007, "Physical Properties of Tissues Relevant to Arterial Ultrasound Imaging and Blood Velocity Measurement," Ultrasound in Medicine and Biology, 33, pp. 1527-1539.